Electron-Impact Spectroscopy: A Versatile Tool for Chemistry

Michael Allan*

Abstract. Selected research projects representative for the applications of the Electron-Impact (EI) techniques in Fribourg are briefly reviewed. Progress made in the development of instrumentation is illustrated with spectra of oxygen and buta-1,3-diene. The following topics are then briefly discussed: *i*) Comparison of triplet- and singlet-excitation energies of a representative aliphatic hydrocarbon (pentane) with the highly strained [1.1.1]propellane and with ethene. *ii*) Electron affinities and virtual orbitals of saturated hydrocarbons with increasing degree of strain: propane, cyclopropane, and [1.1.1]propellane. *iii*) Measurement of absolute cross sections for electronic excitation and comparison with theory. *iv*) Dissociative attachment experiments on dihalosubstitued toluenes providing insight into factors determining the rate of intramolecular charge-transfer in the gas phase.

1. Introduction

Electron-Impact (EI) Spectroscopy has started with the crude Electron-Energy-Loss (EEL) experiments of *Franck* and *Hertz* in 1914, and continued with the first measurements of electron-atom and electron-molecule collision cross sections in the 1930's. Important impetus to electron-collision research was given by the discovery of short-lived negative ions (also called resonances) in electron-molecule collisions in the 1960's and 1970's and the accompanying development of high-resolution instrumentation [1]. The research in this time period was physics-oriented and concentrated on atoms and small molecules.

First applications to chemistry can be traced to the early 70's and evolved along two main lines:
- EEL Spectroscopy was used to observe spin and dipole forbidden transitions in organic compounds. The pioneering work of *Kuppermann et al.* [2] can be considered as a representative example.
- Electron-Transmission (ET) Spectroscopy was used to study temporary negative ions of organic compounds, with the aim to assess the electron affinities,

Correspondence: Prof. Dr. M. Allan
Institut de Chimie Physique de l'Université
Pérolles
CH–1700 Fribourg

the properties of virtual orbitals, and electronic structure of negative ions. Much of the pioneering work has been initiated by *Burrow* and *Jordan* [3].

The results of the early experiments proved very useful for chemistry and a further pursuit of this direction of research was, therefore, initiated in Fribourg in 1981, with emphasis on chemistry-oriented applications and on improvement of instrumentation. The projects currently pursued in Fribourg fall into the following broad categories.

- The capability of the EI techniques to give information on excited states and on virtual orbitals makes it a versatile instrument for the evaluation of the electronic structure of molecules and negative ions and thus an interesting support tool for other areas of chemistry, in particular photochemistry. A recent example is the study of the industrially relevant compound *Tinuvin P* [4], further the study of cyclopropane [5] and other compounds [6][7].
- Study of unimolecular decomposition of negative ions, *e.g.* the recent study of intramolecular competition of dissociation of phenylic and benzenic C–X bonds [8].
- Fundamental studies of electron-molecule collisions, motivated mainly by the interesting effects associated with motion of the nuclei on potential surfaces with extremely short lifetime. Examples are studies of N_2 [9], H_2 [10], HCl [11], and propadiene [12].

The experimental work has often been inspired by, or has subsequently inspired, theoretical studies in other laboratories, which led to the development of important concepts and methods, like the concept of nuclear friction and the development of time-dependent treatment of nuclear dynamics [13][14].

- Measurement of absolute cross sections for electronic excitation in atoms [15] and polyatomic molecules [16] [17]. This experimental work is also accompanied by theoretical work by other research groups, developing, on the one hand, high-precision theory for the electronic excitation in atoms [18], on the other hand, methods for calculating the cross sections even for polyatomic molecules (a formidable task, which could be tackled only very recently, with the development of powerful parallel computers [19][20]). The knowledge of the absolute cross sections for electronic excitation (measured and calculated) is important for the understanding of the numerous technological and environmental systems where electron collisions take place. Examples are atmospheric and interstellar chemistry, ozonizers (the market of which is growing rapidly because of ecological concerns – O_3 is used to bleach paper and disinfect water without chlorine), discharge lamps, and plasmas for surface etching and treatment. Cooperation of theory and experiment is essential for progress in these applications, because theory cannot be developed without reference to reliable experimental data, but theory will finally be needed to calculate the cross sections for free radicals and other transient molecules present in the plasmas but not readily accessible to measurement.
- Attempt has been made to study electron collisions with *van der Waals* clusters [21]. Such studies could be relevant, *e.g.*, for the development of industrial excimer UV lamps, pursued, *e.g.*, by *ABB Switzerland* [22].

Very promising are the recent chemistry-oriented applications of the EI techniques to molecules adsorbed on surfaces and to molecules imbedded in low temperature matrices, which are being pursued in several laboratories around the world [23]. (This direction is, for apparative reasons, not pursued in Fribourg, but cooperation with groups working on surfaces has been initiated with the aim of comparison of surface and gas phase data, which is often not available in sufficiently high quality.)
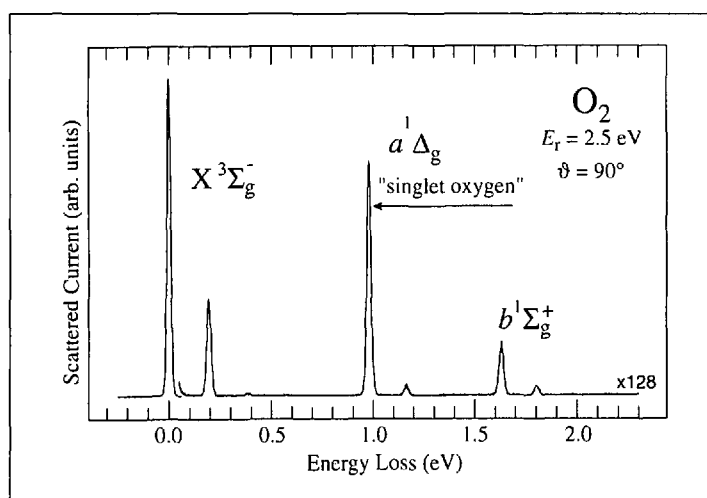
Fig. 1. *EEL Spectrum of O_2 recorded with a low residual energy and at a large scattering angle, where spin-forbidden transitions are enhanced.* The resolution was set to 20 meV to gain sensitivity for this relatively weak signal.
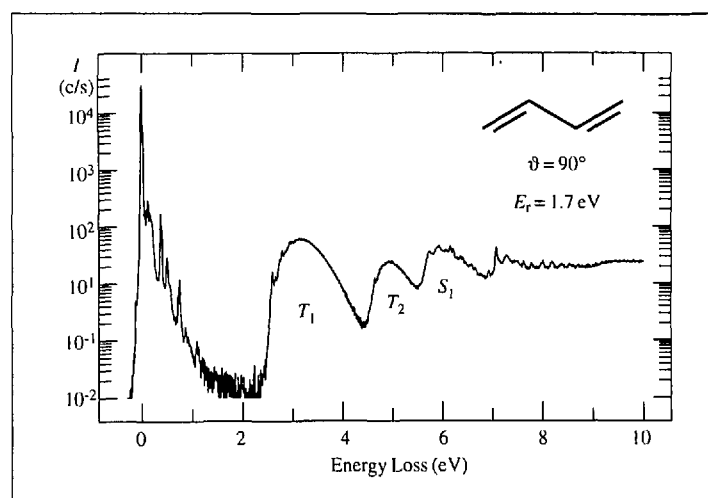

Fig. 2. *Global EEL spectrum of buta-1,3-diene shown on a semilog scale*

The effort in Fribourg is concerned both with development and improvement of instrumentation and with applications to current problems of chemistry. This paper will illustrate some of the instrumental achievements with spectra of well known compounds and review few examples of recent research.

2. Instrumental

2.1. *Trochoidal Electron Spectrometer*

This instrument, described in detail in [6], uses an axial magnetic field to focus the electron beam. It is capable of recording ET spectra, EEL spectra, and excitation functions for specific vibrational and electronic excitation processes, albeit at a fixed scattering angle. The instrument developed in Fribourg introduced several crucial technical improvements, resulting in an overall performance far superior to the 'traditional' electrostatic instruments in terms of very high sensitivity, low sample consumption (useful spectra can be obtained with 50 mg of sample), and sustained performance at very low electron energies. The superior performance is best illustrated by its success in obtaining new data even in small and previously often studied molecules H_2 [10], N_2 [9] (proving very high sensitivity), or HCl [11] (proving excellent performance with very low electron energies). The low sample consumption is important for studies of compounds available only in relatively small quantities, *e.g.*, [1.1.1]propellane [24]. With a high-temperature attachment, this instrument could also measure low-volatility compounds like the fullerene C_{60} [25].

2.2. *Dissociative Electron-Attachment Spectrometer*

By this recently substantially improved [26] instrument, described in more detail in [27], dissociative decay channels of the short-lived anions are studied. The instrument also uses a magnetically focused trochoidal electron monochromator to prepare a quasi-monoenergetic beam of electrons, incorporates an electrostatic analyser for measurement of the fragment anion kinetic energies, and a quadrupole mass filter for fragment mass analysis.

2.3. *Electrostatic Electron Spectrometer*

This is the most recently constructed instrument and is described in [15]. It complements and extends in an important way the trochoidal spectrometer mentioned above. It permits recording of the signal in function of scattering angle, yielding important information on the nature and symmetry of the excited state and of the intermediate negative ion. In its present version, it further permits measurement of *absolute* differential cross sections, which are of crucial importance for comparison with theory, and for applications in plasma and atmospheric chemistry and physics as described above. It offers higher resolution (down to 12 meV, depending on sensitivity) than the trochoidal instrument. This instrument does, however, use much more sample, *ca.* 10 g, are required for an average study of excited states and resonances.

The design of this instrument is essentially 'classical', using hemispherical deflectors for electron-energy selection, but careful choice of materials (Mo for optics, mostly Ti for structural elements), consequent computer control (64 digital-to-an-

alog converters generate the focusing and deflecting voltages), and other technical details result in improved performance, as will be illustrated below.

3. Applications

3.1. *Electron-Energy-Loss Spectroscopy*

The spectrum of O_2, shown in *Fig. 1* illustrates the capacity of EI spectroscopy to detect spin-forbidden transitions, and simultaneously the good resolution/sensitivity ratio and low background obtained with the present instrument in comparison with earlier measurements [28]. It shows clearly the $a^1\Delta_g$ and $b^1\Sigma_g^+$ states and could perhaps be useful in textbooks to visualize the 'singlet oxygen' state.

Fig. 2 shows an EEL spectrum of buta-1,3-diene, also recorded with the electrostatic spectrometer in Fribourg. It agrees well with the earlier spectrum of *Kuppermann* and coworkers [29], but illustrates clearly the improvement in instrumentation. The spectrum is shown on a semilog scale to accommodate the large dynamic range of the signals. It shows the elastic peak at the electron-energy-loss $\Delta E = 0$, followed by peaks due to vibrational excitation. Bands due to triplet- and singlet-excited states can be discerned at higher energy losses. Noteworthy is the large dynamic range of signal intensities covered by the instrument: there are six orders of magnitude between the background level and the height of the elastic peak, even the relatively weak electronic excitation is a factor of hundred above the background. Furthermore, the computer control permits nonlinear adjustments of the beam focusing voltages and, thus, scans over

large energy ranges, yielding global views of the electronic structure of a given molecule. The resolution (ca. 25 meV in combination with the sensitivity of Fig. 2) permits observation of vibrational structure [7], revealing excitation of the C=C and C–C stretch and C–C–C deformation vibrations, in line with the bonding and antibonding nature of the well known π and π* orbitals involved in this transition. Interesting is the similarity of the vibrational structure of the T₁ state with vibrational excitation brought about by a temporary occupation of the π* orbital (shown in Sect. 3.2), pointing out the similarity of

structure changes caused by electron promotion to, and by temporary occupation of, the π* LUMO.

The power of the EEL spectroscopy to show the global view of the excited states of a given molecule is very useful in visualizing the trends in the electronic structure of a series of molecules. This is exemplified in Fig. 3, showing the EEL spectra of three hydrocarbons.

The spectrum of pentane [30] is representative for saturated aliphatic hydrocarbons. The lowest excitation energies are very high. The onsets of the signals under triplet and singlet conditions are similar,

indicating very small singlet-triplet splitting, and thus Rydberg nature of even the lowest excited states [31]. The bands are broad and structureless, resembling the UV-photoelectron bands, in line with the Rydberg assignment. This type of spectra is given by the low-lying HOMO and high-lying valence unoccupied orbitals in aliphatic hydrocarbons.

The lowest triplet band of [1.1.1]propellane [24] is lower than the triplet band of pentane by ca. 3 eV! The substantial singlet-triplet separation of ca. 2.5 eV further points to a compact, valence-like LUMO. The spectra thus illustrate in a very direct manner that the stretched central bond of [1.1.1]propellane is associated with a relatively high-lying HOMO and low-lying valence LUMO. It has been pointed out by Michl [32] that the low-lying σ → σ* triplet is directly related to low homolytic dissociation energy of the central bond. The effect of the bridge bond on electronic structure is so dramatic that it makes the spectrum of propellane resemble the spectrum of ethene, shown for comparison in the lower part of Fig. 4 (see [31] for a general discussion of the ethene spectrum, [17] for the present spectrum).

Interesting is the comparison of band widths of ethene and propellane. The valence-triplet states are of comparable widths, a fact which could be explained by comparable bonding and antibonding character of the HOMO and LUMO orbitals in the two compounds. The valence-singlet bands, however, have dramatically different width in the two compounds: the S₁ band in ethene (it is partially obscured by sharp Rydberg transitions, but the width is well discernible) is wide, comparable to the T₁ band, the S₁ band of propellane is
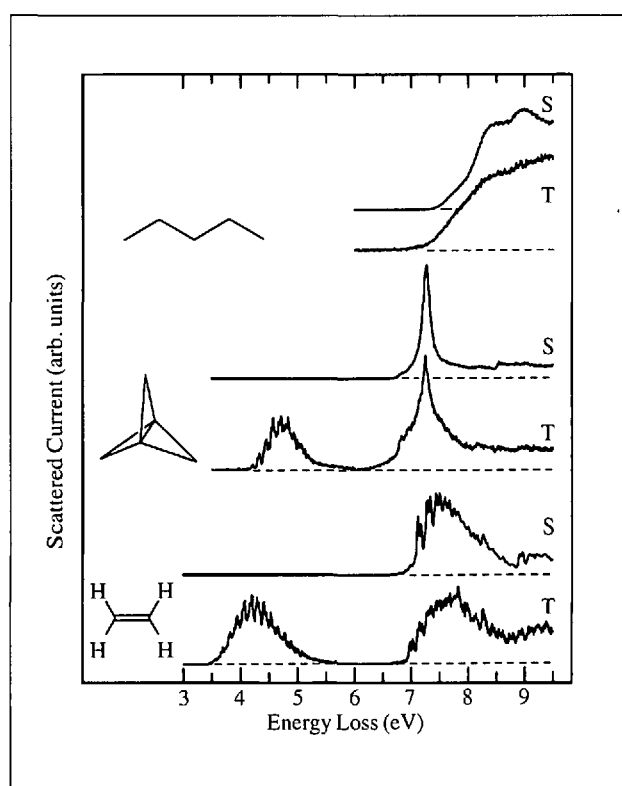
Fig. 3. Comparison of EEL spectra of pentane, [1.1.1]propellane, and ethene. The ethene spectra were recorded with the electrostatic spectrometer, the remaining spectra with the trochoidal spectrometer. The spectra labelled S are recorded under 'singlet conditions', that is with high residual energy and/or low scattering angle and show the dipole allowed transitions. The spectra labelled T are recorded under 'triplet conditions', that is with low residual energy and/or large scattering angle and show both the allowed and the forbidden transitions.
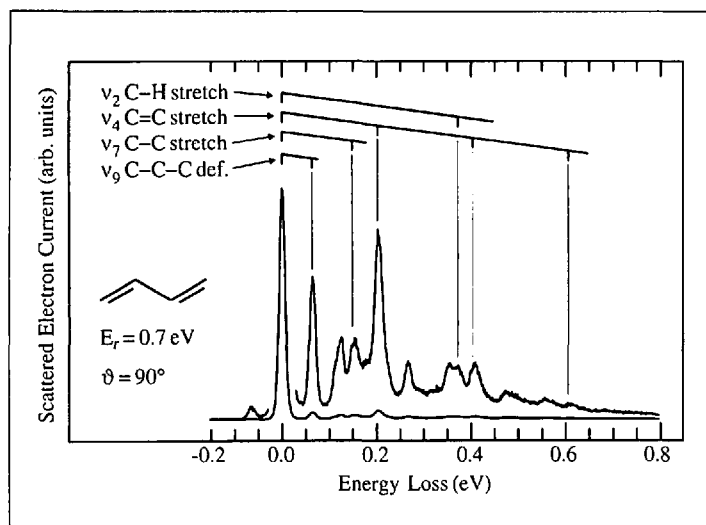

Fig. 4. EEL Spectrum of buta-1,3-diene showing vibrational excitation caused by the π₁* resonance, that is by the temporary occupation of the π₁* LUMO. The resolution is 12 meV.
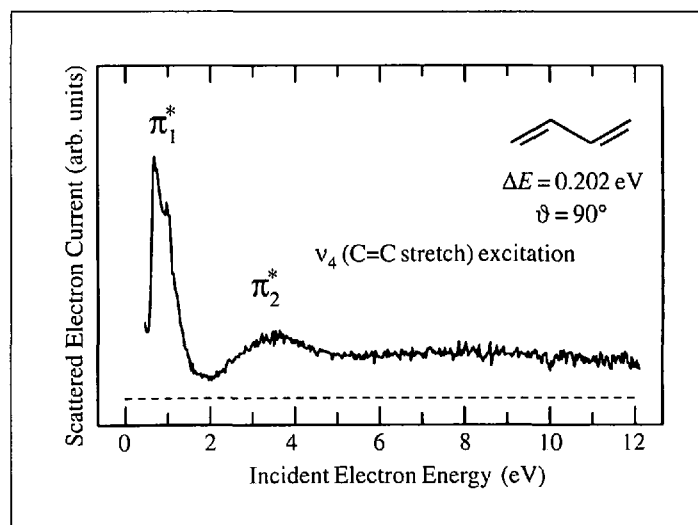
Fig. 5. Excitation function of the C–C stretching vibration in buta-1,3-diene, showing peaks due to the π₁* and π₁* resonances. The signal above 5 eV is probably due to σ* resonances.

unusually narrow. This fact could in part be due to the excitation of twisting vibration in ethene (the S_1 state equilibrium geometry is perpendicular), but a full explanation deserves further study.

3.2. The Study of Resonances

The states of the butadiene negative ion corresponding to temporary occupation of the virtual molecular orbitals were determined to lie at 0.62 eV ($A_u\pi_1^*$ LUMO) and 2.8 eV ($B_g\pi_2^*$) by ET spectroscopy [33]. As already mentioned in the *Introduction*, such states are short-lived due to autodetachment, and are interchangeably called short-lived negative ion states, resonances, or negative ion resonances. The lifetime of the short-lived anion formed by the attachment of an incident electron to the target molecule in resonant scattering is often of the same order of magnitude as the vibrational period. The nuclei of the target molecule, thus, relax on the anion potential surface for a short time, causing vibrational excitation of the target molecule after the anion has eventually decayed back to the neutral molecule through autodetachment. Which vibrations have been excited is thus informative of the nature of the distortion which the molecular skeleton experienced during the lifetime of the negative ion.

Symmetry rules and a very specific distortion caused by distinct antibonding properties of the temporarily occupied orbital generally cause the excitation of only very few vibrations even in polyatomic molecules with many vibrational modes, as has been shown in the pioneering studies on benzene [34] and ethene [35]. This effect is demonstrated here on the vibrational excitation of buta-1,3-diene, shown in *Fig. 4*, caused by temporary occupation of the π_1^* MO. Only few of the 24 vibrational modes are excited. The dominant vibration is C=C stretch, excited by the prolongation of the C=C bond by the temporary occupation of the π_1^* MO. Excitation of a C–C–C deformation vibration is second in intensity, indicating substantial changes of the C–C–C angle in the negative ion. The vibrational excitation spectra are thus very useful for characterizing the nature of the temporarily occupied MO, and for assigning negative ion spectra.

The fact that resonances strongly enhance vibrational excitation can be used to detect them by recording the dependence of exciting some given vibration on incident energy (energy-dependence, ED, spectrum), as shown for the excitation of the C=C stretch vibration in butadiene in *Fig. 5*. The spectrum clearly shows the
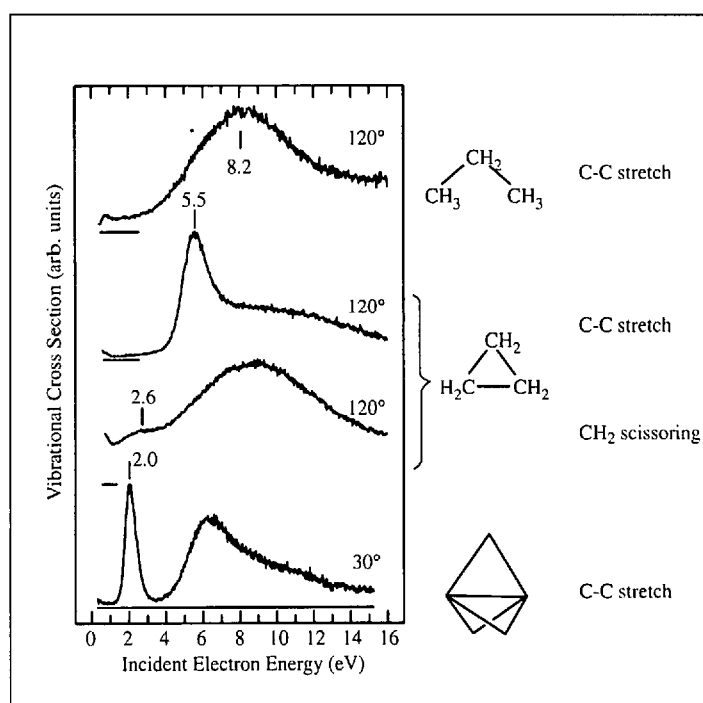

Fig. 6. *Excitation functions of selected vibrations for three saturated hydrocarbons*
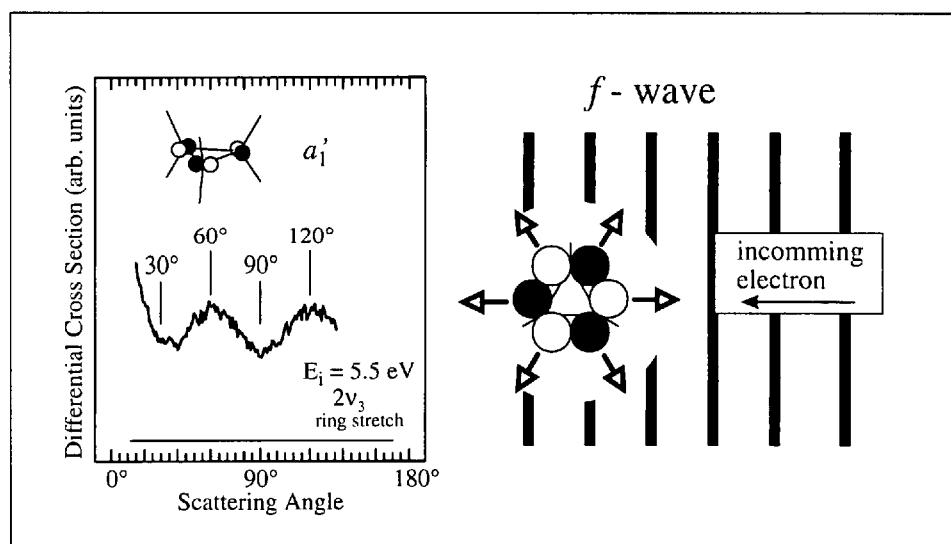

Fig. 7. Left: *Angular distribution of electrons having excited two quanta of the symmetrical ring-stretch vibration of cyclopropane via the 5.5 eV resonance.* Observe the maxima in the forward direction, and at *ca.* 60 and at 120°. Right: *Qualitative explanation of the angular distribution.* The heavy vertical bars signify ridges of the incoming electron's plane wave. The a_1' MO, temporarily occupied in the resonance, is shown schematically in the orientation optimal for electron capture (*i.e.* with optimal overlap of the MO and the free electron plane wave). Short arrows indicate preferred directions of the departing electrons.

π_1^* and π_2^* resonances, and very broad σ^* resonances at higher energies.

This method of determining resonance energies, being essentially a zero background method, has a distinct advantage over the ET spectroscopy, often hindered by the dominant background of nonresonant scattering. This advantage is decisive in particular for broad resonances, which cannot be discerned clearly in the ET spectra. This advantage is exploited in *Fig. 6* to study the often very broad σ^* resonances in saturated hydrocarbons. The top curve shows excitation function of a

C–C stretch vibration of propane. One extremely broad band is observed, with an onset at *ca.* 3 eV, and a maximum around 8 eV. This result indicates one or more (overlapping) broad σ^* resonances at relatively high energies, and a low affinity towards electrons, in line with general chemical experience. Note that ET spectroscopy does not reveal any resonances in the linear saturated hydrocarbons, as exemplified by the ET spectrum of pentane, given in [24]. The shape of the excitation function varies only little with the length of the chain, nearly identical curve was

obtained for ethane [36] and the result in *Fig. 6* is representative of any linear saturated hydrocarbon.

On the other hand the additional strain in cyclopropane has a dramatic effect on the excitation functions [5]. A band peaking at 2.6 eV is observed in the excitation function of the CH_2 scissoring vibration, indicating a sizeable increase of affinity towards electrons. Secondly, a resonance is observed at 5.5 eV in the excitation function of the symmetric C–C stretch vibration, which is unusually narrow for its high energy. The selective excitation of the C–C stretch vibration, the absence of C–H stretch or scissoring vibration, and mainly the observed angular distribution, shown in *Fig. 7*, allows the assignment of this resonance to temporary occupation of a a_1' MO (revising the original assignment of this band in the ET spectrum, see [5]).

Finally, the lowest curve of *Fig. 6* illustrates the dramatic effect which the stretched central bond has on the σ^* energy in [1.1.1]propellane.

3.3. *Measurement of Absolute Differential Cross Sections for Electronic Excitation of Organic Molecules*

The calculation of cross sections for electronic excitation of polyatomic molecules by electron impact has started to become feasible only very recently, due to the availability of very fast computers and to active development of theory. The success of calculations can, however, in general not be assessed because of lack of suitable experimental data. This was recently the case even for such a fundamental molecule as ethene [19]. The instrumentation in Fribourg was able to supply the required data [17], and *Fig. 8* compares the result with the two theoretical

predictions available. The calculated curve of [19] agrees well with the experiment as far as qualitative features are concerned, both curves consist of a relatively broad resonance band preceded by a steep rise above threshold and a shoulder. There are two important quantitative discrepancies, however. First, the $^2(\pi,\pi^{*2})$ $^2B_{3u}$ resonance is calculated at an energy *ca.* 1.5 eV higher than measured. The calculated cross section is further *ca.* two times larger than experimental one in absolute magnitude. This result is not entirely surprising, since the theory uses severe approximations: it does not take into account target polarization, and disregards nuclear motion. The result of the calculation of [37], which took the target polarization partially into account, agrees better with the experiment in terms of absolute magnitude, but exaggerates the size of the threshold shoulder. In conclusion, a fair qualitative agreement of experiment and theory is thus obtained, an encouraging result in view of the size of the theoretical problem of calculating *ab initio* electronically inelastic cross section. Substantial progress will be required, however, before the cross sections for electronic excitation of polyatomic molecules can be calculated quantitatively.

3.4. *Dissociative Attachment*

Dissociative electron transfer in solution

$$RX + e^- \rightleftharpoons R^- + X^-$$

where R⁻ is a carbon-centred radical, X is a halogen, and an electron is taken from an electrode or a suitable donor, is an extensively studied process because of its technological and ecological relevance. This work is concerned with the gas-phase counterpart of this process, the dissociative electron attachment (DA),

$$RX + e^- \rightarrow [RX^-] \rightarrow R^- + X^-$$

where a free electron is captured by an isolated molecule to form a short-lived negative ion [RX⁻] which may then dissociate into a stable X⁻ and a radical R⁻.

We studied the *intramolecular* competition of the two possible C–X dissociation processes in the dihalogen compounds 1–6, carrying simultaneously a halogen connected directly to the benzene ring (phenylic C–X bond) and the other separated by a methylene group (benzylic C–X bond) [8].
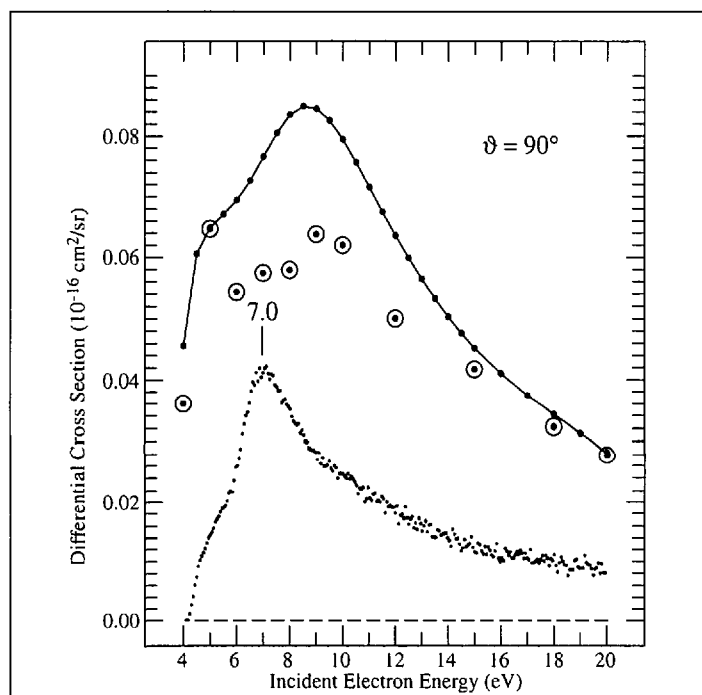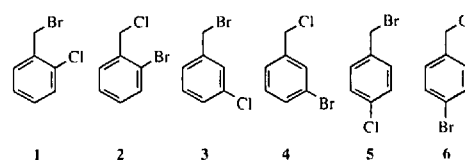

Fig. 8. *Differential cross section for the excitation of the lowest triplet state of ethene at 90° as a function of incident electron energy. Small dots: the experimental cross section, recorded near the maximum of the triplet EL band (see Fig. 3), but normalized to reflect the rovibrationally integrated cross section. Larger dots connected by straight lines represent the result of the calculation of Sun et al. [19], encircled dots results of Rescigno and Schneider [37].*
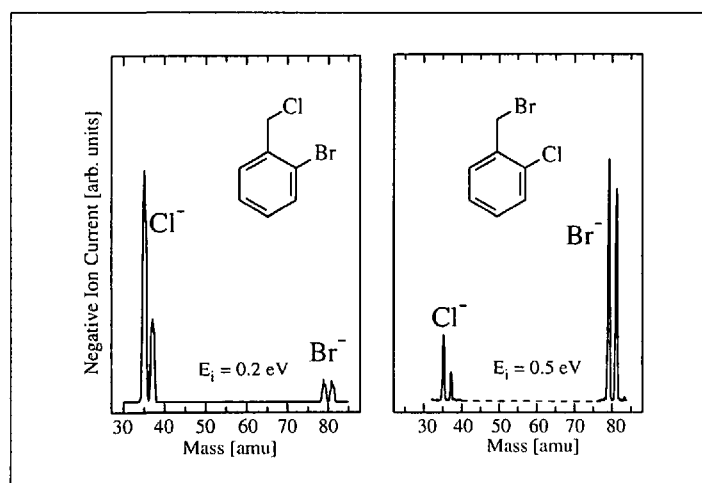

Fig. 9. *Negative-ion mass spectra obtained with incident electron energies indicated, for 1 and 2*

The experiment shows that an attachment of slow electrons (0–0.8 eV) results in X⁻ production for all above compounds. Mass spectra recorded at incident energies within this low energy DA band (example is shown in *Fig. 9*) show that the signal of the benzylic X⁻ is five to tenfold higher than the yield of phenylic X⁻ for all substitution patterns and irrespective of whether X⁻ is Cl⁻ or Br⁻.

This observation is interpreted as a result of both energy and symmetry effects. The loss of benzylic X⁻ is, on the one hand, favored energetically as a result of the weaker benzylic C–X bond. On the other hand, the effect of symmetry appears to be important, because the selectivity of the dissociation remains preserved even when Cl and Br are interchanged, that is even when the energetics is substantially changed because C–Br bond is weaker than C–Cl bond.

The symmetry argument is based on the fact that the molecules **1–6** may be approximately viewed as possessing a local plane of symmetry in the benzene ring. The phenylic halogen is lying in this plane, the intramolecular electron transfer from the π^* into the corresponding σ^* orbital and the ensuing DA are symmetry-forbidden. The benzylic C–X bond is rotated out of the local symmetry plane for steric reasons, permitting efficient π^*/σ^* coupling, intramolecular electron transfer and dissociation. This situation is illustrated by the potential curves and orbital diagrams in *Fig. 10*. It shows that the σ^*_{C-Cl} does not appreciably mix with the π^* MO's of the benzene ring, but the mixing of σ^*_{C-Br} and π^* is substantial, resulting in a dissociative potential curve. *Fig. 10* also illustrates the intramolecular electron transfer by showing that the lowest MO of the anion is essentially a benzene π^* at low C–Br distances, but becomes progressively a σ^*_{C-Br} MO as R_{C-Br} is increased.

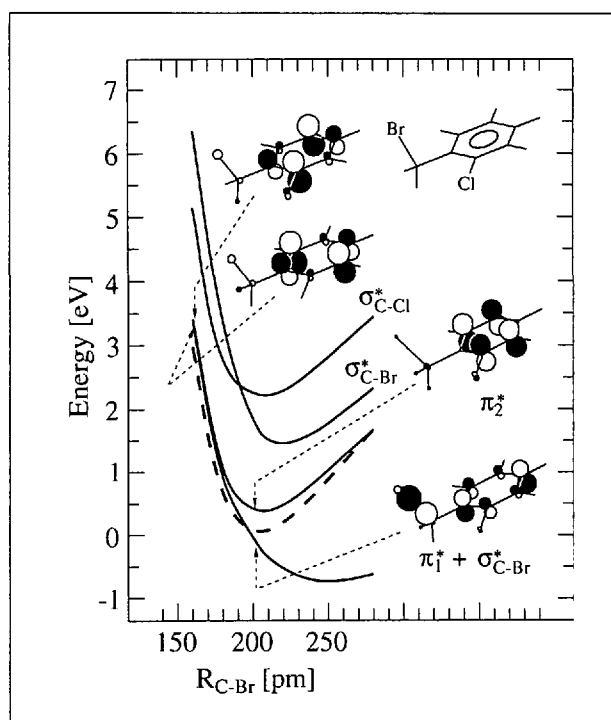Fig. 10. *Potential energy of the compound* **1** (dashed line) *and its radical anion* (solid lines) *as function of the C–Cl distance, obtained from a HF/LANL1DZ calculation with application of* Koopmans' *theorem* (see [8] for details). Schematic diagrams of the singly occupied orbitals for the lowest two states of the anion were drawn using the program MOPLOT [38]. The MO diagrams are given for two internuclear separations, as indicated by arrows.

[1] G. J. Schulz, *Rev. Mod. Phys.* **1973**, *45*, 423.

[2] A. Kupperman, W M. Flicker, O. A. Mosher, *Chem. Rev.* **1979**, *79*, 77.

[3] K. D. Jordan, P. D. Burrow, *Chem. Rev.* **1987**, *87*, 557.

[4] M. Allan, K. Asmis, C. Bulliard, E. Haselbach, P Suppan, *Helv. Chim. Acta* **1993**, *76*, 993.

[5] M. Allan. *J. Am. Chem. Soc.* **1993**, *115*, 6418.

[6] M. Allan, *J. Electron. Spectrosc.* **1989**, *48*, 219.

[7] M. Allan, Proceedings of the XVth IUPAC Symposium on Photochemistry, Prague, July 1994, in print.

[8] Ch. Bulliard, M. Allan, E. Haselbach, *J. Phys. Chem.* **1994**, in press.

[9] M. Allan, *J. Phys. B: At., Mol. Phys.* **1985**, *18*, 4511.

[10] M. Allan, *J. Phys. B: At., Mol. Phys.* **1985**, *18*, L451.

[11] O. Schafer, M. Allan, *J. Phys. B: At., Mol. Opt. Phys.* **1991**, *24*, 3069.

[12] M. Allan, *J. Chem. Phys.* **1994**, *100*, 5588.

[13] W. Domcke, *Phys. Rep.* **1991**, *208*, 97-188.

[14] P. L. Gertitschke, W. Domcke, in press.

[15] M. Allan, *J. Phys. B: At., Mol. Opt. Phys.* **1992**, *25*, 1559.

[16] M. Allan, *J. Chem. Phys.* **1994**, *101*, 844.

[17] M. Allan, *Chem. Phys. Lett.* **1994**, *225*, 156.

[18] W. C. Fon, K. Ratnavelu, P. M. J. Sawey, *J. Phys. B: At., Mol. Opt. Phys.* **1993**, *26*, L555.

[19] Q. Sun, C. Winstead, V. McKoy, M. A. P. Lima, *J. Chem. Phys.* **1992**, *96*, 3531.

[20] C. Winstead, Q. Sun, V. McKoy, *J. Chem. Phys.* **1992**, *97*, 9483.

[21] M. Allan, *J. Phys. B: At. Mol. Opt. Phys.* **1993**, *26*, L73.

[22] U. Kogelschatz, *Appl. Surf. Sci.* **1992**, *54*, 410.

[23] P. Swiderek, M.-J. Fraser, M. Michaud, L. Sanche, *J. Chem. Phys.* **1994**, *100*, 70; D. Antic, D. E. David, J. Michl, contributions to the XVth IUPAC Symposium on Photochemistry, Prague, July 1994; R. Azria, Y. LeCoat, J.-P. Ziesel, J.-P. Guillotin, B. Mharzi, M. Tronc, *Chem. Phys. Lett.* **1994**, *220*, 417; M. Meinke, E. Illenberger, *J. Phys. Chem.* **1994**, *98*, 6601.

[24] O. Schafer, M. Allan, G. Szeimies, M. Sanktjohanser, *J. Am. Chem. Soc.* **1992**, *114*, 8180.

[25] Ch. Bulliard, M. Allan, S. Leach, *Chem. Phys. Lett.* **1993**, *209*, 434.

[26] C. Bulliard, Ph.D. thesis, Fribourg 1994.

[27] Y. Pariat, M. Allan, *Int. J. Mass Spectrom. Ion Processes* **1991**, *103*, 181.

[28] S. F. Wong, M. J. W. Boness, G. J. Schulz, *Phys. Rev. Lett.* **1973**, *31*, 969.

[29] O. A. Mosher, W. M. Flicker, A. Kuppermann, *Chem. Phys. Lett.* **1973**, *19*, 332.

[30] K. Asmis, S. El houar, M. Allan, unpublished.

[31] M. B. Robin, 'Higher Excited States of Polyatomic Molecules', Academic Press, Orlando, 1985, Vol. III.

[32] J. Michl, *Acc. Chem. Res.* **1990**, *23*, 127.

[33] K. D. Jordan, P. D. Burrow, *Acc. Chem. Res.* **1978**, *11*, 341.

[34] S. F. Wong, G. J. Schulz, *Phys. Rev. Lett.* **1975**, *35*, 1429.

[35] I. C. Walker, A. Stamatovic, S. F. Wong, *J. Chem. Phys.* **1978**, *69*, 5532.

[36] L. Boesten, H. Tanaka, M. Kubos, H. Sato, M. Kimura, M. A. Dillon, D. Spence. *J. Phys B: At., Mol. Opt. Phys.* **1990**, *23*, 1905.

[37] T. N. Rescigno, B. I. Schneider, *Phys. Rev. A* **1992**, *45*, 2894.

[38] A. Schmelzer, E. Haselbach, *Helv. Chim. Acta* **1971**, *54*, 1299. Improved and modernized version of *T. Bally, B. Albrecht* and *S. Matzinger*.